www.czasopisma.pan.pl PAN www.journals.pan.pl

Opto-Electronics Review 25 (2017) 290–295

Contents lists available at ScienceDirect

Opto-Electronics Review

journal homepage: http://www.journals.elsevier.com/opto-electronics review

Electrically tunable long-period fiber gratings with low-birefringence liquid crystal near the turn-around point

A. Czapla[a,*], W.J. Bock[b], T.R. Woliński[a], P. Mikulic[b], R. Dąbrowski[c], E. Nowinowski-Kruszelnicki[c]

[a] Faculty of Physics, Warsaw University of Technology, 75 Koszykowa St., 00-662 Warsaw, Poland
[b] Centre de Recherche en Photonique, Université du Québec en Outaouais, 101 Rue Saint-Jean-Bosco, Gatineau, QC J8X 3X7, Canada
[c] Military University of Technology, 2 Kaliskiego St., 00-908 Warsaw, Poland

ARTICLE INFO

Article history:
Received 2 February 2017
Received in revised form 25 March 2017
Accepted 4 July 2017
Available online 28 September 2017

Keywords:
Long-period fiber grating
Liquid crystal
Sensors
Electric field

ABSTRACT

In this work, an electrically tunable long-period fiber grating (LPFG) coated with liquid crystal layer (LC) is presented. As a LC layer, a prototype low-birefringence 1550A LC mixture was chosen. As a LPFG host, two types of gratings were studied: the LPFGs based on a standard telecommunication fiber, produced by an electric arc technique with a period of 222 μm, and the LPFGs based on a boron co-doped fiber written by a UV technique with a period of 226.8 μm. The relatively short period of these gratings allowed exploiting unique sensing properties of the attenuation bands associated with modes close to the turn-around point. Experiments carried out showed that for the UV-induced LPFG with a LC layer, on the powered state the attenuation band could be offset from the attenuation band measured in the unpowered state by almost 130 nm. When the arc-induced LPFG was coated with the LC, the depth of the attenuation band could be efficiently controlled by applying an external E-field. Additionally, all experimental results obtained in this work were supported by the theoretical analysis based on a model developed with Optigrating v.4.2 software.

1. Introduction

The development of a long-period fiber grating (LPFG) has had a significant impact on research and optical communications network and fiber optic sensing system. Compared to other optical devices, LPFGs have several unique advantages such as low-level back-reflection, low insertion losses and a compact construction (the grating is an intrinsic fiber device) [1–5]. LPFGs can be found in a variety of applications in optical communications such as gain-flattening filters for erbium-doped fiber amplifiers (EDFAs) [1], wavelength division multiplexing (WDM) systems [2], and wavelength-selective optical fiber polarizer components [10,11]. LPFGs could also be successfully incorporated into a fiber-optic sensing system, since they provide a mechanism for producing a wavelength-dependent attenuation in the transmission spectrum which can be controlled by external effects [3,4].

The LPFG is a structure made by periodic (typically with period Λ of 100 to 700 μm) modulation of refractive index within the core of a single-mode optical fiber. The modulation induces coupling between the core mode (LP_{01}) and the co-propagating symmetric cladding modes (LP_{0m}, $m = 2, 3, 4\ldots$), resulting in the emergence of a series of resonance attenuation peaks in a LPFG's transmission spectrum. These resonant wavelengths λ_{res}^{m} are defined by:

$$\lambda_{res}^{m} = (n_{eff,co} - n_{eff,cl}^{m})\Lambda, \quad (1)$$

where $n_{eff,co}$ and $n_{eff,cl}^{m}$ are the effective refractive indices of the fundamental core mode and mth cladding mode, respectively. The value of $n_{eff,cl}^{m}$ dependent upon the refractive index (RI) of the external medium n_{ext} [4] (increase of n_{ext} increases $n_{eff,cl}^{m}$). Thanks to this feature, changes in the n_{ext} can be simply detected by measuring the shift of the resonant wavelength in the LPFG transmission spectrum. This effect gets stronger when n_{ext} is closer to that of the cladding (typically made of fused silica), however, it does not occur when it is higher than RI of the fiber clad [3]. To overcome this limitation, the LPFGs coating with a high-refractive index (HRI) layer where presented [4]. They provide the shift of the highest RI sensitivity range towards its lower values. Such modification depends on layer thickness and its optical properties, mainly RI. Moreover, if the layer material selected is sensitive to a specific parameter, highly sensitive and specific devices can be obtained, including, e.g., a chemo-sensors and bio-sensors [6,7]. LPFG sensitivity can be also enhanced greatly if the grating period and layer RI are optimized in a way to operate at a point called turn around point (TAP)

* Corresponding author.
E-mail address: czapla@if.wp.edu.pl (A. Czapla).

http://dx.doi.org/10.1016/j.opelre.2017.07.002
1896-3757/

on phase matching curves of these gratings. Thus, a generation of dual resonant bands, which shows sensitivities of the opposite sign, can be observed in the LPFG transmission spectrum. TAP LPFGs are well known for their ultrahigh sensitivity to external parameters [8–10].

The sensing properties of LPFGs can be also improved by merging them with liquid crystals (LC). LCs are self-organized anisotropic materials that exhibit high electro- and thermo-optic effects associated with their birefringence, their dielectric anisotropy and thermal dependence of their RIs [11–15]. Consequently, LPFGs combined with LCs, known as LC-LPFGs, have been seen as promising structures for creating a new platform for tunable fiber devices; e.g., thanks to the electro-optical properties of the LC materials, the LC-LPFG will demonstrate electric sensitivity in addition to the sensitivities of the grating itself.

One of the first examples of LPFG tuning by using LC was demonstrated by Duhem et al. [16]. They proposed a modulation of the attenuation band intensity based on the electrical switching of a nematic liquid crystal (NLC) around a photoinduced LPFG. Yin et al. presented a device based on an ultrathin LPFG etched by hydrofluoric acid (HF) which was surrounded by a dye-doped NLC for tuning the resonant wavelength [17]. A cascade structure of LPFGs with LC as the surrounding medium was proposed furthermore by H-R Kim et al. [18] for arbitrary loss filters that could compensate a non-uniform optical gain in an EDFA. Also noteworthy are the results presented in Ref. [19] where LPFGs, based on the SMF-28 and photonic crystal fibers (PCF), surrounded by a low-birefringence (LB) 1550 LC mixture were thermally and electrically tuned. In this work, a special glass capillary with five holes was used, where metal wires were placed in four holes (serving as electrodes) while the LPFG was introduced in the central hole and, then, filled with the LC. Later, the idea of a coated LPFG with a thin LC layer (in the order of 1 μm) was brought forward by Luo et al. [20]. The host LPFG used in this research was fabricated by a CO2 laser irradiation, and a medium-birefringence (MB) LC was employed as a LC layer. The experimental results along with the theoretical analysis presented there showed that efficient thermal tuning can be achieved for such a LC-LPFG design (up to 80 nm). Later, in Ref. [21] the electric and thermal tuning of the UV-induced LPFG combined with low-birefringence (LB) LC mixtures was presented. In this work, two different methods were used in order to obtain a LC coating on the LPFG: placing the LPFG inside a capillary and filling it with LC, or directly coating the bare LPFG with a thin LC layer. It was shown that the LPFG, when enhanced with an external LB LC layer, exhibits two different temperature sensitivities which depend on the temperature range of operation (corresponding with a nematic and an isotropic LC phases). The "switching" functionality of this LC-LPFG around the LC clearing temperature *Tc* was also observed (useful, for example, in warning systems). For the grating coating with a LC layer the electric induced shift of the attenuation band (up to 11 nm) was achieved, as well. In Ref. [22] it was demonstrated that a temperature compensation effect could be obtained in the LPFG by a proper choice of the LC layer. In Ref. [23], the phenomenon of the dual-resonance was exploited for the first time to measure LC-LPFG structure thermal and electric field responses.

In this work the use of a hybrid LC-LPFG is aimed at taking advantage of the 1550A LB nematic LC serving as a thin layer on the LPFG bare. The LPFGs were fabricated on a boron co-doped photosensitive fiber (Fibercore PS1250/1500) by two methods: UV-irradiation method and arc-induced technique (detail description of this method can be find in Refs. [10,24]). To further explore the benefits of the host gratings we chose the relatively short periods of 226.8 μm (for the UV-induces LPFG) and 222 μm (for the arc-induced LPFG). This type of gratings offered the possibility of coupling the optical power to the higher-order cladding modes and for the UV-induced LPFG leads also to a phenomenon of dual resonance. These properties are exploited to measure LC-LPFGs electric field responses. Effective electric tuning for the UV-induced LPFG with 1550ALC layer was obtaind since the investigated attenuation band was close to TAP. For such a LC-LPFG design, in the powered state the attenuation band was offset from the one measured in the off-voltage state by almost 130 nm. Electrical tuning of the LC-LPFG close to TAP was also achieved for the arc-induced LPFG host. In this case a fast switching on/off of the attenuation band in the LC-LPFG transmission spectrum for the powered/unpowered states was obtained. Simultaneously, all experimental results obtained in this work were supported with a basis on a model developed with Optigrating v.4.2 software.

2. Materials and experimental procedure

In this experiment, we used a commercially available boron co-doped photosensitive fiber (Fibercore PS1250/1500) as a host fiber. The LPFGs were fabricated by two methods. We produced the grating with a period of 222 μm by electric arc discharge. The grating was fabricated with a period of 226.8 μm by using the UV Eximer laser irradiation (*PulseMaster GSI Lumonics* emitting at a wavelength of 248 nm). The details of the LPFGs fabrication procedure can be found in Refs. [10,24].

As an external layer for the LPFG, a prototype LC mixture 1550A was chosen (synthesized at Military University of Technology, Warsaw, Poland). The refractive indices' thermal characteristics (measured at 589 nm) for this LC are presented in Fig. 1a). Table 1 provides a summary of the electro-optical properties for 1550A LC.

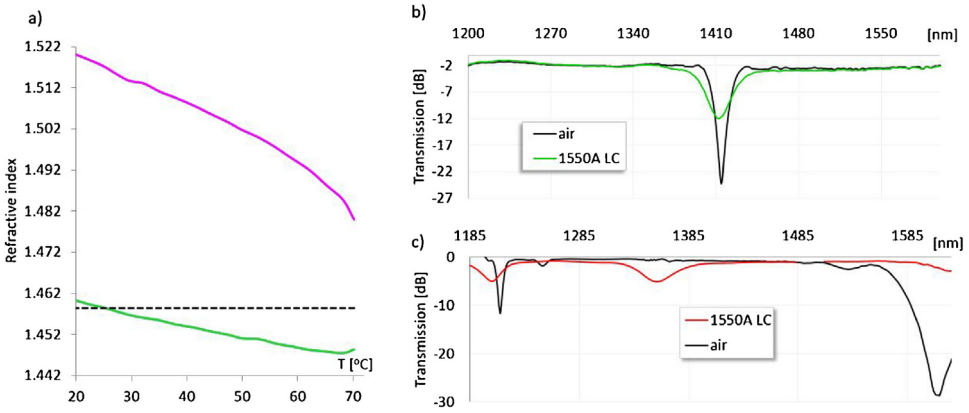

Fig. 1. a) The 1550A LC thermal dependencies of ordinary n_o (green line), extraordinary n_e (red line), as well silica glass n_{cl} (dashed line) refractive indices measured at wavelength of 589 nm. b) Transmission spectra of the arc-induced LPFG (b) and UV-induced LPFG (c) with and without LC layer.

Table 1
Electro-optical properties of the 1550A LC (measured at wavelength of 589 nm and at 25 °C).

Clearing temperature, T_C[°C]	Ordinary RI, n_o	Extraordinary RI, n_e	Birefringence, Δn	Dielectric anisotropy, $\Delta\varepsilon$
71	1.4592	1.5168	0.0594	>0

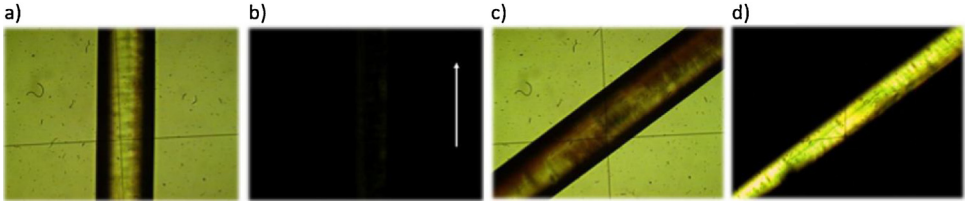

Fig. 2. LPFG with the LC layer placed in the polarizing optical microscope observed in not polarized light [a),c)] and when the LC-LPFG axis was perpendicular to the first polarizer axis b) and at 45° to the crossed polarizers d).

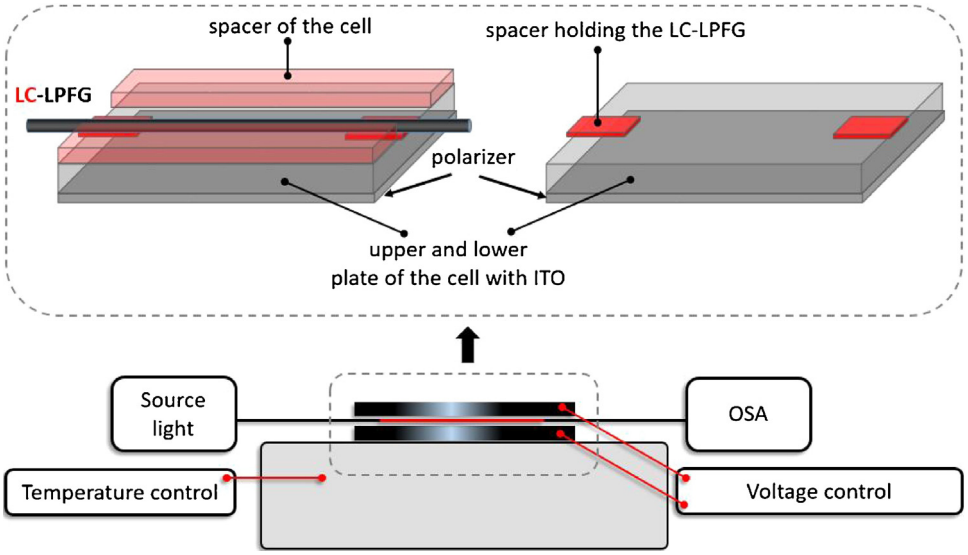

Fig. 3. Experimental setup to investigate spectral properties of LC-LPFGs under the influence of E-field.

To provide a better alignment of the LC molecules, the LPFGs were first rubbed several times along the fiber axis using cotton swabs. Then LC-LPFGs were fabricated by forming a thin LC layer on the bare grating. The surface tension of the LC facilitates the creation of a quasi-uniform coat on the LPFG, resulting in a thin (micron scale) overlay. Transmission spectra of tested LPFGs, measured in with and without LC layers are presented in Fig. 1b) and c).

The degree of ordering of the LC orientation has a significant effect on the LC RI value and is of prime importance. When the geometry of the host fiber is considered in this context, for the UV-induced LPFG the overall impact to the LC alignment can be negligible. In general, the arc-induced LPFGs can be characterized by the structural deformation. However, for the arc-induced LPFG studied within this work, no variations of the fiber cladding dimension were observed [24]. It can, therefore be assumed that this effect should not have an impact on the LC alignment. To verify this statement the LC layer alignment was examined under a polarizing optical microscope [25]. The procedure of this process was as follows: first, the LC-LPFG axis was parallel to the first polarizer axis (see Fig. 2b) – the white arrow represents the polarizer axis direction), and then rotated about 45° [(see Fig. 2d)]. As can be noticed, when the LC-LPFG axis was parallel to the first polarizer axis the light almost complete faded out [(Fig. 2b)]. This direct observation confirms that a nearly planar alignment has been obtained.

The LC-LPFGs were tested under the influence of E-field by placing them on a specially designed housing unit (Fig. 3). Two plates with ITO served as electrodes which were separated from each other by 135 μm. Electrical control was achieved within a range between 0 V/μm to 4 V/μm. It is also worth noting that this housing unit prevents LC-LPFG cross-sensitivity to physical parameters such as stress and bending, as well providing temperature stabilization (a module Peltier was placed at the house unit bottom providing this way a temperature control). The transmission spectra of the sample were investigated with input light launched from an Agilent 83437 broadband light source and the output signal was analyzed by an Optical Spectrum Analyzer (OSA).

3. Simulation of the LC-LPFG

To better understand the LC-LPFG principles of operation, we developed a model of the thin-LC layer-coated LPFG. The software tool chosen for this purpose was OptiGrating v.4.2, which calculates the interactions of modes in the gratings using the coupled mode theory. In our model the electrical switching effect in the attenuation bands of the LC-LPFG transmission spectrum occurs thanks to the cladding modes' transition (described in details elsewhere [23]).

In Table 2 parameters used in the simulation for the study host LPFGs are summarized. The fiber model is based on the manufacturer's datasheets for the fiber used in the experimental work (boron co-doped photosensitive Fibercore PS1250/1500 fiber). Gratings periods and lengths were determined during the

Table 2
Specification of the LPFG models.

Fiber parameters			
n_{co}	n_{cl}	r_{co}	r_{cl}
1.44933	1.44403	3.97	59.3

Grating parameters					
UV-induced LPFG			Arc-induced LPFG		
period	length	RI modulation Δn_{co}	period	length	RI modulation Δn_{co}
226.8 μm	35,000	2×10^{-4}	222 μm		

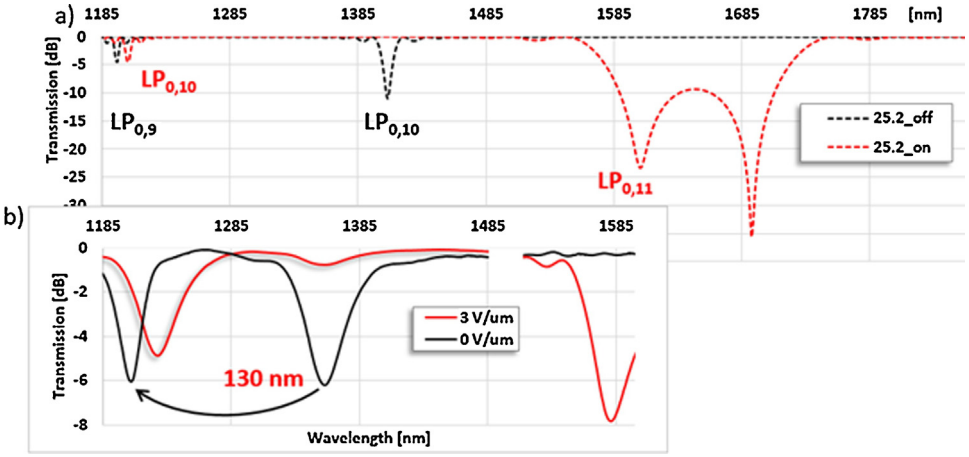

Fig. 4. Simulated a) and experimental measured b) transmission spectra the unpowered and powered states for the UV-induced LPFG with period of 226.8 μm with 1550A LC layer.

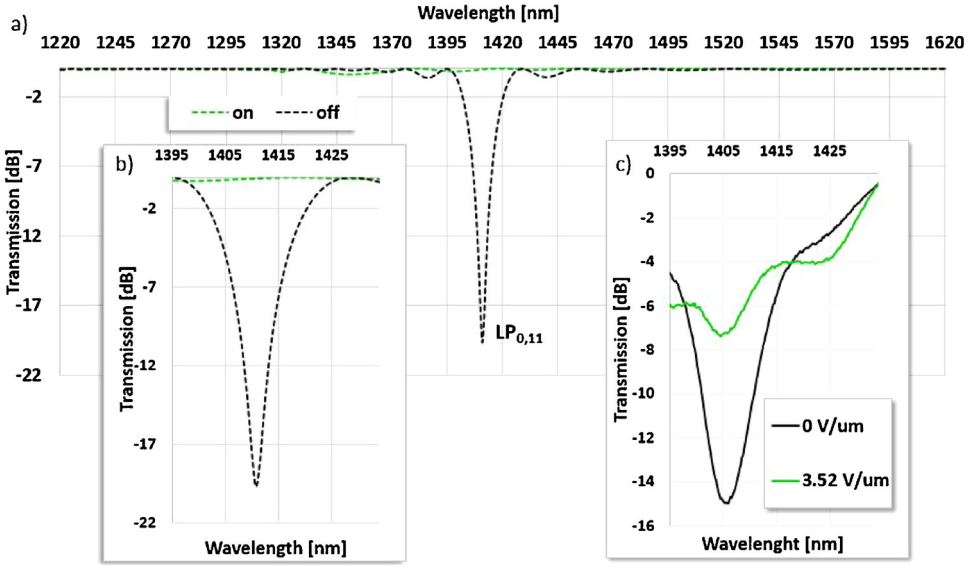

Fig. 5. Simulated a),b) measured c) transmission spectra in the unpowered and powered states for the arc-induced LPFG with period of 222 μm coated with 1550A LC layer.

fabrication process. It is important to noticed that for the arc-induced LPFGs the host fiber can be tapered. However, it was presented that for the arc-induced LPFG, like the design studied here, no modification of its diameter was measured [24]. Thus, in the simulations, it was assumed that during the grating fabrication process based on the arc technique the structural deformation did not occur. The precision of the LC layer thickness measurement under the experimental work gives us the possibility to determine its value to be of a few micrometers. The more exact value of the LC layer thickness was defined by fitting the LC-LPFG transmission spectra as measured vs.E-field with data from the simulation. We arrived at estimated LC layer thickness of 1.8 μm and 2.1 μm for the UV-induced LPFG and arc-induced LPFG grating, respectively.

4. Results and discussion

To examine the impact of the E-field on the LC-LPFG spectral properties, a series of experiments was conducted when a short period of the grating (226.8 μm and 222 μm) was chosen. This type of LPFGs exhibits enhanced sensitivity. This is since, in their

transmission spectrum, we can observe attenuation bands which are associated with higher-order modes. Higher order modes are showing greater sensitivity to any external perturbation. In addition, when the coupling of such a higher-order mode occurs near the TAP, the attenuation band contains dual resonant peaks at two separate wavelength values. Consequently, by operating at wavelengths near to the mode phase-matching turning point, higher sensitivity of the LC-LPFG to the electric field should be observed.

The high electric tuning ability was obtained for the UV-induce LPFG coated with 1550A LC. By fitting both experimental and simulated outcomes, the 1550A LC layers thickness could be estimated to be of as 1.8 μm. Results shown in Fig. 4 indicate that an E-field can induce significant changes in the transmission spectrum. In the off-voltage state two attenuation bands are visible [Fig. 4b)]. Thanks to the performed simulation [presented in Fig. 4a)], it could be established that the measured attenuation bands at 1207 nm and at 1359 nm results from the coupling of the $LP_{0,9}$ and $LP_{0,10}$ modes, respectively. By applying the E-field to the sample, the RI of the LC layer increases. Therefore, the reorganization of the modes occurs. Thus, in the powered state the attenuation band corresponding with the $LP_{0,10}$ is offset from the attenuation band measured in the unpowered state by almost 130 nm. The attenuation band associated with the $LP_{0,9}$ mode is no longer visible in the spectral range of interest. In addition, by increasing the E-field, an additional attenuation band appears in the LC-LPFG transmission spectrum. Comparing the simulated and experimental transmission spectrum, it can be deduced that this attenuation band corresponds with the $LP_{0,11}$ which is close to TAP.

Electric tuning of the LC-LPFG close to TAP was also achieved for the arc-induced LPFG host. This grating was coated with the 1550A LC layer, as well. The thickness of the LC layer was estimated to be of 2.1 μm. Figure 5 shows that the depth of the attenuation band was reduced significantly in the presence of an E-field. Through the theoretical work, it was found that the attenuation band measured in the unpowered state results from coupling of the $LP_{0,11}$ mode. This result can be interpreted by the fact that the change in the LC layer under the influence of an E-field gives a value of the RI for which the modes are very close to the TAP where significant decrease of the visibility of the attenuation bands should be expected. In other words, the mode that should take the $LP_{0,11}$ mode's place (precisely the $LP_{0,12}$ mode) was not yet formed in the LC-LPFG transmission spectrum.

5. Conclusions

This work reports on the investigation of advanced tunable photonic components known as liquid crystal long-period fiber gratings (LC-LPFGs). The major contribution of this research is presenting new electric tuning effects achieved in LC-LPFGs due to the electro-optic properties of the 1550A LB LC layer. We also demonstrated that the electrical spectral tuning ability of this design of LC-LPFG can be improved significantly by choosing an appropriate grating period which gives the possibility of measuring the attenuation bands associated with higher-order modes. In addition, if these modes are close to the TAP, a dual-resonant phenomenon can be exploited in term of its electric sensitivity.

The significant change in the transmission spectrum of the UV-induced LPFG with 1550A LC layer was measured in the presence of an E-field. In the powered state, the attenuation band was offset from the attenuation band measured in the unpowered state by almost 130 nm. This effect occurs thanks to the fact that the measured attenuation band was close to the TAP. Electric tuning of the LC-LPFG close to TAP was also achieved for the arc-induced LPFG host coated with 1550A LC layer, as well. In this case the depth of the attenuation band was reduced significantly in the presence of an E-field. Such high variations in amplitude can be exploited in the same manner as the wavelength shift in sensor applications. It is suspected that the attenuation band measured in the powered state is very close to the TAP where a significant decrease of the visibility of the attenuation bands should be expected. Simultaneously, to better understand the underlying principles of operation, we developed a model of the thin-layer-coated LC-LPFG (see [23]). The software tool chosen for modelling this concept was OptiGrating v.4.2. The calculations performed allowed us to qualitatively analyze the LC-LPFG from a theoretical perspective.

Acknowledgements

This work was supported by the Natural Sciences and Engineering Research Council of Canada and by the Canada Research Chairs Program. The authors are also grateful to the Fonds Québécois de la Recherche sur la Nature et les Technologies (FQRNT).

References

[1] O. Frazão, G. Rego, M. Lima, A. Teixeira, F.M. Araújo, P. André, J.F. Rocha, H.M. Salgado, EDFA gain flattening using long-period fiber gratings based on the electric arc technique, Proc. Lond. Commun. Symp. 2001 (2001) 55–57.
[2] X.J. Gu, Wavelength-division multiplexing isolation fiber filter and light source using cascaded long-period fiber gratings, Opt. Lett. 23 (7) (1998) 509–510.
[3] X. Shu, L. Zhang, I. Bennion, Sensitivity characteristics of long-period fiber gratings, J. Lightwave Technol. 20 (2) (2002) 255–266.
[4] G. Rego, A review of refractometric sensors based on long period fibre gratings, Sci. World J. 2013 (2013) 913418.
[5] M. Szeląg, P. Lesiak, D. Budaszewski, M. Chychłowski, T.R. Woliński, Investigation of strain induced effect on linear shape fiber Bragg grating embedded in composite material, Photonic Lett. Poland 8 (3) (2016) 88–90.
[6] E. Brzozowska, M. Śmietana, M. Koba, S. Górska, K. Pawlik, A. Gamian, W.J. Bock, Recognition of bacterial lipopolysaccharide using bacteriophage-adhesin-coated long-period gratings, Biosens. Bioelectron. 67 (2015) 93–99.
[7] M. Konstantaki, A. Klini, D. Anglos, S. Pissadakis, An ethanol vapor detection probe based on a ZnO nanorod coated optical fiber long period grating, Opt. Express 20 (8) (2012) 8472–8484.
[8] I. Del Villar, Ultrahigh-sensitivity sensors based on thin-film coated long period gratings with reduced diameter, in transition mode and near the dispersion turning point, Opt. Express 23 (7) (2015) 8389–8398.
[9] S.M. Tripathi, W.J. Bock, A. Kumar, P. Mikulic, Temperature insensitive high-precision refractive-index sensor using two concatenated dual-resonance long-period gratings, Opt. Lett. 38 (10) (2013) 1666–1668.
[10] M. Smietana, W.J. Bock, P. Mikulic, J. Chen, Tuned pressure sensitivity of dual resonant long-period gratings written in boron co-doped optical fiber, J. Lightwave Technol. 30 (8) (2012) 1080–1084.
[11] I.C. Khoo, S.T. Wu, Optics and Nonlinear Optics of Liquid Crystals, World Scientific Publ., 1997.
[12] J. Li, S.-T. Wu, Extended Cauchy equations for the refractive indices of liquid crystals, J. Appl. Phys. 95 (3) (2004) 896–901.
[13] D. Budaszewski, A.K. Srivastava, A.M.W. Tam, T.R. Woliński, V.G. Chigrinov, H.-S. Kwok, Photoaligned ferroelectric liquid crystals in microchannels, Opt. Lett. 39 (16) (2014) 4679–4682.
[14] M.S. Chychłowski, S. Ertman, E. Nowinowski-Kruszelnicki, T.R. Woliński, Escaped radial and planar liquid crystal orientation inside capillaries, Mol. Cryst. Liq. Cryst. 553 (1) (2012) 127–132.
[15] M.S. Chychłowskia, O. Yaroshchuk, R. Kravchuk, T.R. Woliński, Liquid crystal alignment in cylindrical microcapillaries, Opto-Electron. Rev. 20 (2012) 47–52.
[16] O. Duhem, J.F. Henniont, M. Warenghem, M. Douay, L. Rivoallan, Long-period fiber gratings modulation by liquid crystal cladding, Proc. 6th IEEE Conf. on Telecommunications (1998) 195–196.
[17] S. Yin, K.-W. Chung, X. Zhu, A novel all-optic tunable long-period grating using a unique double-cladding layer, Opt. Commun. 196 (1–6) (2001) 181–186.
[18] H.R. Kim, Y. Kim, Y. Jeong, S. Baek, Y.W. Lee, B. Lee, S.D. Lee, Suppression of the cladding mode interference in cascade long-period fiber gratings with liquid crystal cladding, Mol. Cryst. Liq. Cryst. 413 (2004) 399–406.
[19] A. Czapla, T.R. Woliński, W.J. Bock, E. Nowinowski-Kruszelnicki, R. Dąbrowski, J. Wójcik, Longperiod fiber gratings with low-birefringence liquid crystal, Mol. Cryst. Liq. Cryst. 502 (1) (2009) 65–76.
[20] H.X. Luo Li, S. Li, J. Chen, Analysis of temperature-dependent mode transition in nanosized liquid crystal layer-coated long period gratings, Appl. Opt. 48 (25) (2009) F95–F100.
[21] A. Czapla, W.J. Bock, T.R. Woliński, R. Dabrowski, E. Nowinowski-Kruszelnicki, Tuning cladding mode propagation mechanisms in liquid crystal long-period fiber gratings, J. Lightwave Technol. 30 (8) (2012) 1201–1207.

[22] A. Czapla, W.J. Bock, T.R. Wolinski, Designing sensing properties of the long-period fiber grating coated with the liquid crystal layers, Proc. SPIE 8421 (2012) 84215H.
[23] A. Czapla, W.J. Bock, T.R. Woliński, P. Mikulic, E. Nowinowski-Kruszelnicki, R. Dąbrowski, Improving the electric field sensing capabilities of the long-period fiber grating coated with a liquid crystal layer, Opt. Express 24 (5) (2016) 5662–5673.
[24] M. Śmietana, W.J. Bock, P. Mikulic, J. Chen, Increasing sensitivity of arc-induced long-period gratings – pushing the fabrication technique toward its limits, Meas. Sci. Technol. 22 (2011) 015201.
[25] J.G. Delly, The Michel-Lévy interference color chart. The microscopist's magical color key, (Modern Microscopy, 2003 http://www.modernmicroscopy.com/main.asp?article=15.